

## Supporting Information

# Morphology Dependent Light-Induced Photoluminescence Enhancement of CsPbBr<sub>3</sub> Microcrystals

Xin Ye<sup>‡</sup>, Cuicui Li<sup>‡</sup>, Jinke Jiang, Xiaoxin Zheng, Quangxiang Han, Qinglian Lin, Yang Liu\* and  
Xutang Tao\*

State Key Laboratory of Crystal Materials, Institute of Crystal Materials, Shandong University,  
Jinan 250100, China.

Email: liuyangicm@edu.cn, txt@sdu.edu.cn

<sup>‡</sup> These authors contributed equally to this work.

## 1. Experimental Section

### 1.1 Chemicals and materials

**Preparation of CsPbBr<sub>3</sub> Powders.** The CsPbBr<sub>3</sub> Powders were prepared by grinding CsPbBr<sub>3</sub> crystals in an agate mortar. The CsPbBr<sub>3</sub> crystals were synthesized by a homemade thermal field-elevating melt growth technique as reported in our previous work.<sup>1, 2</sup> Halides and lead salts, including cesium bromide CsBr (99.999%) and PbBr<sub>2</sub> (99.999%) were purchased from the Sigma-Aldrich. PbBr<sub>2</sub> and CsBr (5 g and 2.899 g,) were fully mixed before being placed in an ampule. Then the ampule was placed in the growth furnace. In order to ensure an oxygen-free environment during crystal growth, the growth furnace chamber was subjected to three vacuuming and purging steps with argon gas. The high temperature zone and cold temperature zone were heated up to 620 °C and 450 °C, respectively. First, the ampule was located in the hot zone for 12 h. Then the oven was moved upward at the speed of 4 mm/h to cool the melting materials. Then the CsPbBr<sub>3</sub> crystals crystallized from the melt. When the crystallization process finished, the temperature of furnace cooled to room temperature at a rate of 5–15 °C/h.

### 1.2 Material characterization

**Microscope Measurement.** Optical images were obtained using a Nikon ELIPSE Ni inverted microscope system equipped with a Nikon LV-EPILED reflector and a Nikon DS-Ri2 photographic system. Fluorescence images were obtained using a Nikon Ti-U Inverted Microscope System equipped with a Nikon C-SHG 1 mercury lamp. The exposure time to acquire a bright photo on a fluorescence microscope for CsPbBr<sub>3</sub> cubes is as short as 30 ms and 100 ms for CsPbBr<sub>3</sub> prisms.

**Electron Microscopy Measurement.** Scanning electron microscopy (SEM) was obtained by a Hitachi S-4800 ultrahigh resolution (UHR) field emission (FE) scanning electron microscope, and the pictures were taken at an accelerating voltage of 5.0 kV.

**Powder X-ray Diffraction.** The X-ray diffraction pattern was collected with an X'Pert3 Powder&XRK-900 X-ray diffractometer with Cu K $\alpha$  radiation ( $\lambda = 1.54056 \text{ \AA}$ ) in a room-temperature atmospheric environment.

**PL spectra measurement.** Steady-state fluorescence measurements were performed with an Edinburgh Instruments FLS980 spectrometer. Fluorescence quantum yields were determined with the FLS980 spectrometer using optically dense samples in an integrating sphere. Fluorescence lifetimes were measured by time-correlated single-photon counting (TCSPC) at the FLS980 spectrometer using pulsed laser diodes at 375 nm (EPL-375) as the excitation source.

**Absorption spectra measurement.** The absorption spectroscopy was carried out using a conventional UV/Vis spectrometer (Hitachi U-4100) equipped with an integrating sphere over the spectral range of 300–800 nm.

## 2. Data

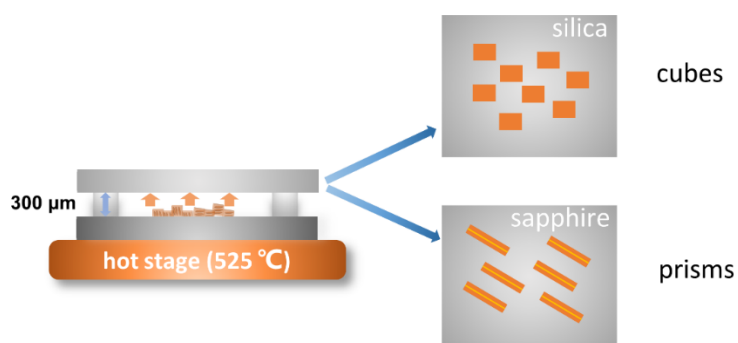


Fig. S1 Schematic diagram of the growth of CsPbBr<sub>3</sub> cubes and prisms on different substrates.

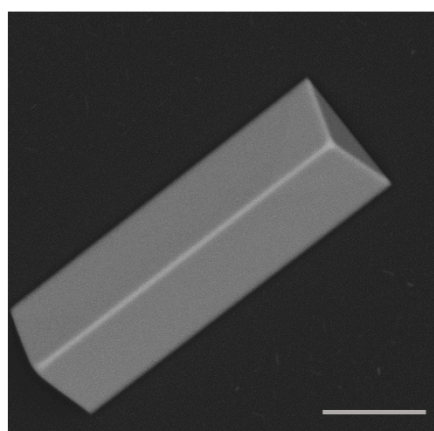


Fig. S2 Tilted SEM image of CsPbBr<sub>3</sub> prism. (Scale bar: 5 μm).

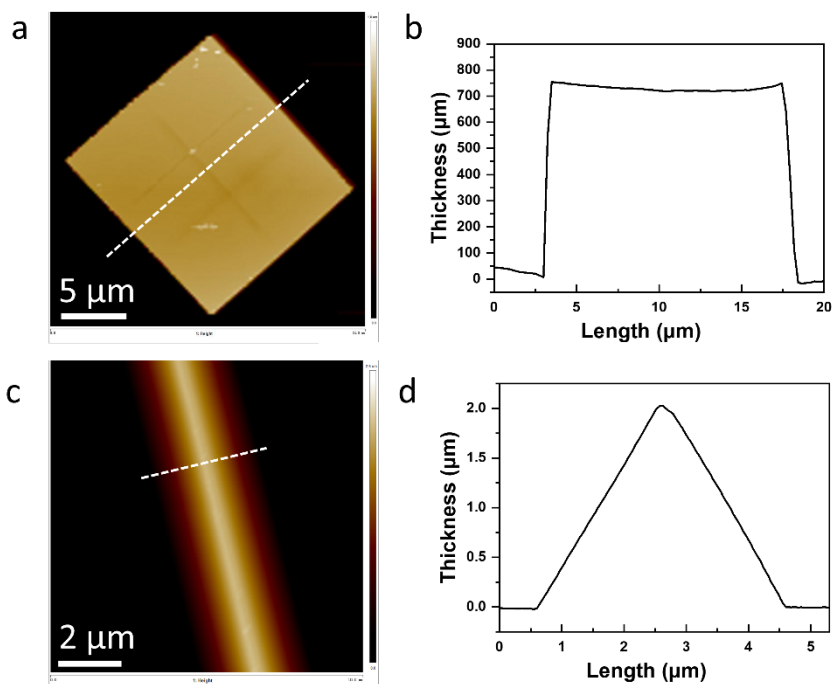


Fig. S3 (a and c) AFM images and cross-section thickness profile of CsPbBr<sub>3</sub> cubes and prisms. (Scale bar: 5 μm for a, 2 μm for c).

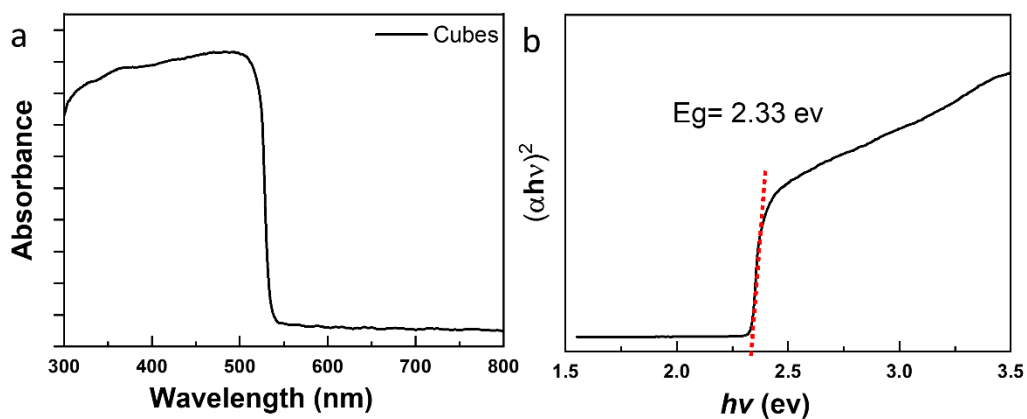


Fig. S4 (a) Absorption spectra of CsPbBr<sub>3</sub> cubes. (b) Absorbance versus photon energy and the determined bandgap  $E_g$ .

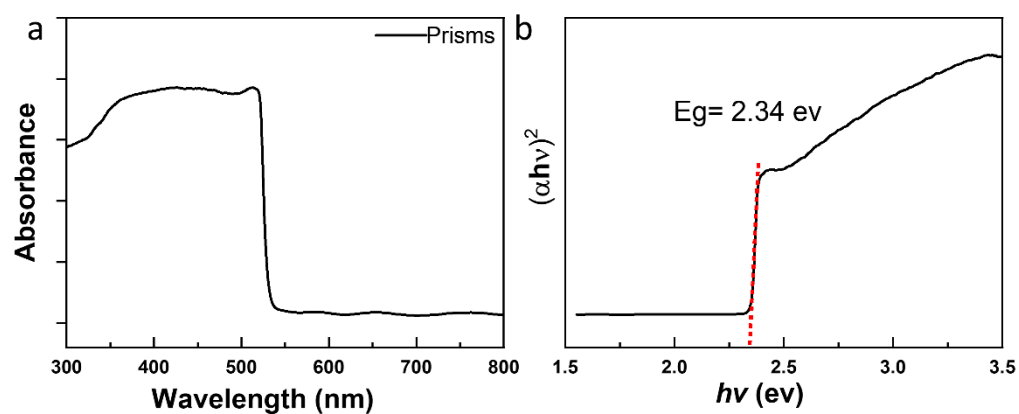


Fig. S5 (a) Absorption spectra of CsPbBr<sub>3</sub> prisms. (b) Absorbance versus photon energy and the determined bandgap  $E_g$ .

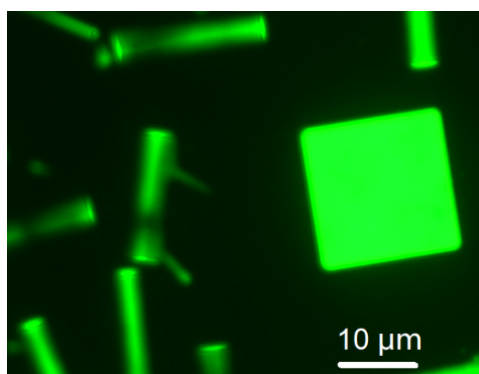


Fig. S6 Fluorescence microscope images of CsPbBr<sub>3</sub> cubes and prisms.

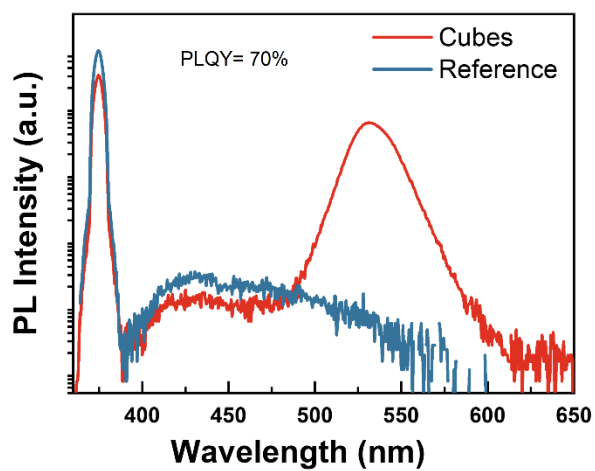


Fig. S7 PLQY of CsPbBr<sub>3</sub> cubes.

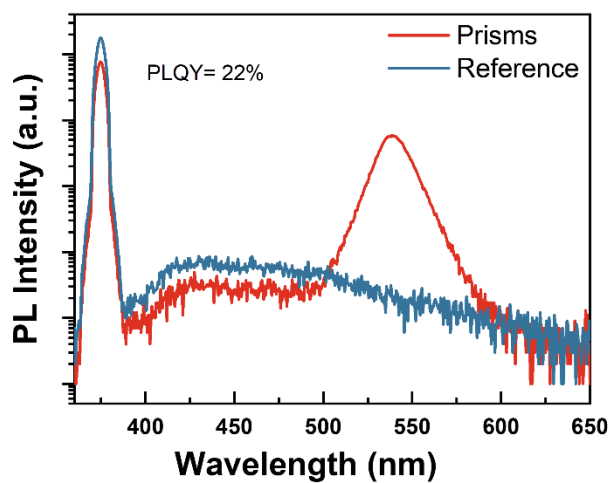


Fig. S8 PLQY of CsPbBr<sub>3</sub> prisms.

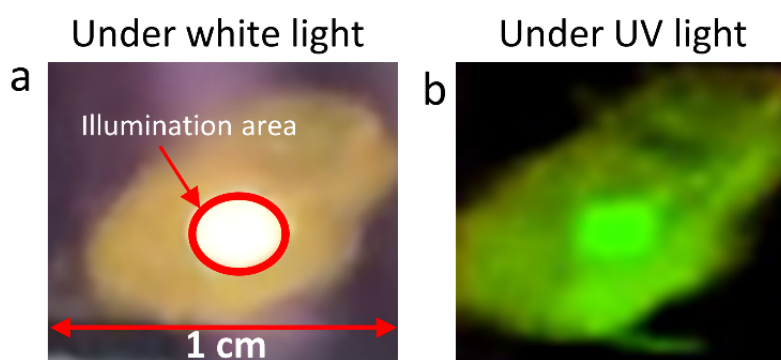


Fig. S9 Photograph of CsPbBr<sub>3</sub> crystals. (a) The crystals are partially illuminated under white light. The red circle indicates the illumination area. (b) The crystals are under UV light.

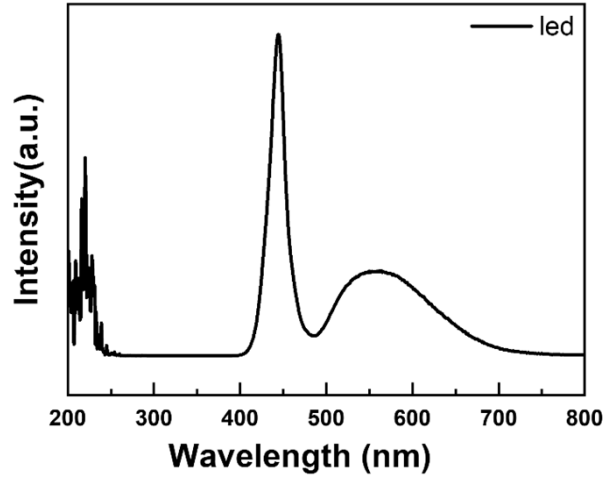


Fig. S10 Luminescence spectrum of the white LED.

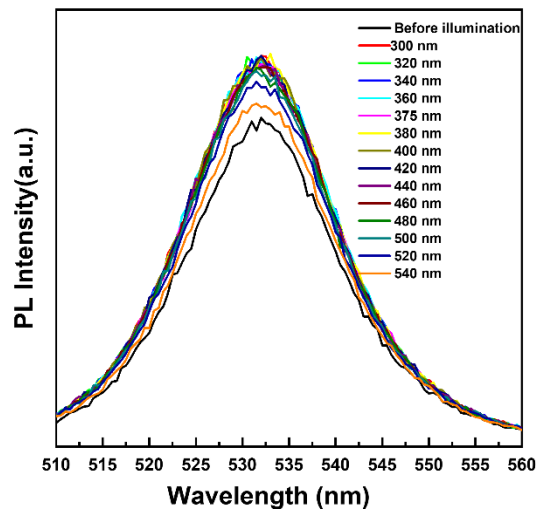


Fig. S11 PL spectra of CsPbBr<sub>3</sub> cubes after illumination with various wavelengths.

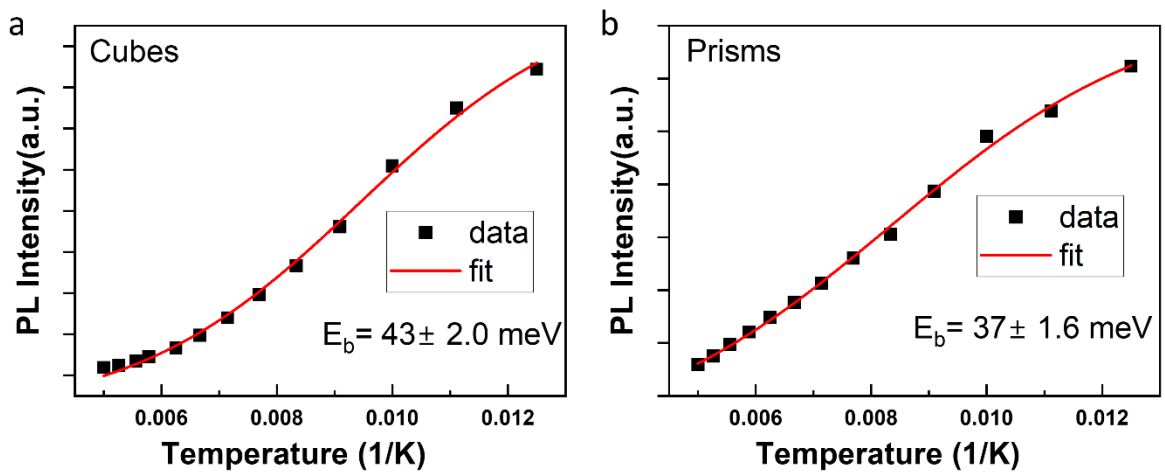


Fig. S12 PL emission intensity plotted as a function of temperature. The squares are experiment data and the red lines are fitting curves. The exciton binding energy can be fitted using equations,

$$I = \frac{I_0}{1 + A e^{-E_b/k_B T}}$$
, in which  $I_0$  is the PL emission intensity at  $T= 0$  K,  $A$  is temperature-independent constant,  $E_b$  is the exciton binding energy of  $\pm$ , and  $k_B$  is the Boltzmann constant. The exciton binding energy ( $E_b$ ) is extracted as  $43 \pm 2.0$  meV and  $37 \pm 1.6$  meV for cubes and prisms respectively from the data fitting process.

### References

1. S. Cui, T. Zhu, L. Zhang, X. Ye, Q. Han, C. Ge, Q. Guo, X. Zheng, Q. Lin and C. Li, *Advanced Optical Materials*, 2022, 2102355.
2. P. Zhang, Q. Sun, Y. Xu, X. Li, L. Liu, G. Zhang and X. Tao, *Crystal Growth & Design*, 2020, 20, 2424-2431.